18TH WORLD CONFERENCE ON EARTHQUAKE ENGINEERING
WCEE2024
MILAN

MILAN, ITALY
30TH JUNE - 5TH JULY 2024
www.wcee2024.it

SURROGATE MODELING FOR SEISMIC FRAGILITY PREDICTION OF MASONRY INFILLED RC FRAMES

R. Chelapramkandy[1], J. Ghosh[2] & F. Freddi[3]

[1] Indian Institute of Technology Bombay, Mumbai, India, rifanc@iitb.ac.in

[2] Indian Institute of Technology Bombay, Mumbai, India

[3] University College London, London, United Kingdom

Abstract: *Reinforced concrete (RC) frames with masonry infills have continued to remain a popular construction typology across the globe, including regions characterized by moderate to high seismic activity. Owing to the brittle nature of the masonry infills, their influence on the seismic analysis and design of framed structures has been typically neglected. However, scientific literature and field reconnaissance surveys indicate that the strength, stiffness, and distribution of masonry infills within RC frames can significantly influence their seismic performance. Typical finite element modeling of masonry infills within RC frames for nonlinear time history analysis comprises of single or multiple struts modeling approaches that require detailed information on the characteristic back-bone curve of the masonry infill. However, past studies report considerable variability associated with the material parameters of masonry infills (such as strength and elasticity) that may affect the seismic response and fragility of RC framed structures. This paper proposes a novel framework that develops parameterized seismic fragility functions for infilled RC frames conditioned on critical infill material parameters in addition to ground motion intensity. Unlike typical unidimensional fragility functions, the parameterized multidimensional fragility models offer flexibility to efficiently asses the influence of infill material parameters on seismic vulnerability. Such models are developed in the present study through a systematic approach rooted in statistical learning techniques. Initially, an experimental design is devised that considers an optimal combination of infill material parameters for computer simulations. Next, the seismic response from these simulations is obtained to develop surrogate models that predict engineering demand parameters (e.g., interstory drifts) as a function of infill material parameters and ground motion intensity. Lastly, the seismic demands obtained from the surrogate models are compared with seismic capacity estimates to generate the parameterized seismic fragility functions. The proposed methodology is applied to a case-study low-ductility RC frame with masonry infills to underline the gain in computational efficiency and accuracy for seismic response and vulnerability prediction.*

1. Introduction

Masonry infilled reinforced concrete (RC) frames represent a conventional construction practice followed worldwide, including seismically active areas (Cavaleri and Di Trapani, 2014; Mosalam and Günay, 2015; Sattar and Liel, 2016). However, owing to the brittle nature of the masonry infills, they are typically neglected during the seismic analysis and design stages (Crisafulli *et al.,* 2000; Dolšek and Fajfar, 2008). On the other hand, several studies in recent literature indicate that the strength and stiffness of masonry infills can substantially influence the seismic performance of RC frames (Blasi *et al*., 2018; Campione *et al*., 2015; Martinelli *et al*., 2015; Mucedero *et al*., 2023). Moreover, RC frames constructed prior to the implementation of the modern-day seismic design codes are typically characterized by low ductility and, hence, are significantly vulnerable to seismic loads (Rao *et al*., 2020; T. Rossetto and Elnashai, 2003). The complex interaction

between such low-ductility RC frame and the masonry infills may significantly magnify their vulnerability, especially in cases where the infills are distributed irregularly (Cavaleri and Di Trapani, 2014; Dolšek and Fajfar, 2008). On the other hand, there are instances where the presence of masonry infills enhances the seismic performance of the RC frames (Cavaleri and Di Trapani, 2014; Dolšek and Fajfar, 2008).

The contribution of the masonry infills to the strength and stiffness of the structure can be simulated using different finite element (FE) modeling strategies. Such approaches can be typically divided into micro- and macro-modeling methods (Crisafulli *et al*., 2000; Di Sarno *et al*., 2021; Sattar and Liel, 2016; Wu *et al*., 2022). Micro-models provide a detailed representation of the infill walls and offer a precise representation of the response under lateral loads. However, this strategy requires significant computational effort and is often deemed infeasible for multi-story, multi-bay buildings (Sattar and Liel, 2016). In contrast, macro-models use simplified representations of the infills, often based on replacing the infill with one or more struts in the diagonal direction (Crisafulli *et al.,* 2000); this helps in reducing the computational runtime, which is the primary reason for adopting the macro-modeling method. It is worth noting that such models require incorporating the highly nonlinear behavior of the masonry infill to correctly simulate the response during high-intensity seismic events (Dolšek and Fajfar, 2008).

Advanced seismic performance assessment procedures, such as the Performance-Based Earthquake Engineering (PBEE) framework, are mainly used for evaluating the seismic performance of large or critical structures such as nuclear power plants and bridges. In contrast, they are seldom used on mid-rise buildings due to the high computational demand required (Esteghamati and Flint, 2021). On the other hand, masonry infills can have different geometries (*e.g.,* thickness, aspect ratios), varying levels of confinement, and can be formed by bricks of different materials (*e.g.,* clay, concrete, stone), along with different shapes (*e.g.,* solid or hollow masonry units), and dimensions. Generalizing the contribution of masonry infills through advanced assessment procedures would require accounting for a large set of parameters, leading to a substantial computational effort. In this context, surrogate modeling offers an effective alternative to provide comprehensive seismic performance assessment, simultaneously limiting the computational demand required (Esteghamati and Flint, 2021).

The present study proposes a novel framework to develop parameterized seismic fragility functions using surrogate modeling techniques for masonry infilled RC frames. Unlike typical unidimensional fragility functions conditioned only on the seismic intensity measure (*IM*), the parameterized multidimensional fragility functions are also conditioned on masonry infill parameters, such as cracking strength and shear modulus of masonry infill. A three-story, three-bay, low-ductility RC frame infilled with masonry is selected for case study purposes. Firstly, this study identifies and defines the typical range of variation in the material properties of the masonry infills that characterize the nonlinear force-displacement back-bone curve of masonry infill. Next, OpenSees is used to develop a two-dimensional FE model of the case study structure. Subsequently, Nonlinear time-history analyses (NLTHAs) were carried out on a limited number of models with masonry infill whose back-bone curves are developed based on the samples of infills' material properties obtained using statistical sampling techniques. Based on the demand parameters obtained from the NLTHAs, a surrogate model for the seismic demand conditioned on the infill parameters and *IM* is developed using regression analysis. Subsequently, nonlinear static pushover analysis is performed on the infilled RC frame to obtain the capacity estimates of the structure, and successively, the parameterized fragility functions are derived for the structure. The novel framework proposed in this study can be extended to additional parameters to develop comprehensive and generalized parameterized multidimensional fragility functions for seismic performance evaluation and vulnerability assessment.

2. Surrogate modeling

The use of FE models and numerical simulations is a popular method followed for several decades to seek solutions to engineering problems. However, in some situations, these models are computationally demanding due to the complex representation of the physical phenomena. Moreover, several engineering problems, such as those providing risk estimates against natural hazards, require large sets of computer simulations to incorporate the uncertainties of the problem, making it computationally demanding (Alizadeh *et al.,* 2020). In such situations, surrogate modeling techniques emerge as better alternative. In such techniques, computer simulations of complex engineering problems are performed on a limited number of models whose parameter estimates are carefully selected using an experimental design. Subsequently, mathematical models using the

surrogate modeling technique are used to characterize the output of the limited number of computer simulations. This mathematical model can then be used as a substitute for the complex engineering problem to map inputs to the outputs (Esteghamati and Flint, 2021).

The present study develops a parameterized multidimensional seismic fragility function that depends on the material properties of the masonry infill in addition to the seismic *IM*. For instance, if *y* is the engineering demand parameter (*e.g.,* maximum interstory drift ratio) of a building after a nonlinear analysis, and **x** = {**p,***IM*} be the input vector. The input vector **x** includes *IM* and the parameters characterizing the material properties of the masonry infill, such as strength and elasticity parameters, represented by vector **p** = {p_1,p_2,…, p_m}. The surrogate demand model develops a mathematical relationship between vector **x** and *y*. Let the actual relation between **x** and *y* be:

$$y = f(\mathbf{x}) \tag{1}$$

and the mathematical model g(**x**) developed using the surrogate modeling technique to predict the response output is expressed as follows:

$$y = g(\mathbf{x}) + \varepsilon \tag{2}$$

where ε is a normal random variable with a mean zero representing the total homoscedastic error from lack-of-fit. The details of the design of experiments and the surrogate model adopted in this study are described in the following paragraphs.

This study uses the Latin Hypercube design of experiments to sample the material parameters of the masonry infill (McKay *et al*., 1979). The range of each material parameter of the infills is divided into *n* intervals having equal marginal probability. Successively, one value from each interval is sampled for each material parameter in such a way that it maximizes the minimum distance between the material parameter pairs of *n* samples, producing an *n*×*m* design matrix, where *m* is the number of material parameters considered. Subsequently, each ground motion is paired with *n* different rows of the design matrix. Now, *n* number of nonlinear time-history analysis is performed on the building modeled with *n*×*m* design points, and *n* different seismic response output is estimated.

The next step is the development of surrogate demand models using the set of estimated output **y** and input parameters **x**. Among the different surrogate models available, this study uses a polynomial response surface model with first-order polynomial to fit the input and output parameters as shown in Equation (3):

$$\hat{y} = \beta_0 + \sum_{i=1}^{r} \beta_i x_i \tag{3}$$

where $\hat{y}$ is the predicted seismic response; β_0, β_1,…, β_r are the regression coefficients obtained after fitting the input parameters and output response parameter obtained from the NLTHAs performed on a limited number of models; and x_1, x_2,…,x_r, are the predictors.

3. Case study building

This research uses a three-story, three-bay, low-ductility RC frame designed only for gravity loads for the case study. This structure is representative of low-ductility RC frames in the US and many other seismic regions worldwide and has been selected due to the availability of experimental results at global (Bracci *et al.,* 1995) and local levels (Aycardi *et al.,* 1994), allowing the validation of the numerical models (Freddi *et al*., 2013, 2017, 2021). The beams in the structure are typically designed to resist bending moments, whereas columns are designed to resist the axial forces without specific considerations on the seismic detailing (Elwood and Moehle, 2005; Freddi *et al.,* 2021; Paulay and Priestley, 1992). Post-earthquake reconnaissance missions have shown that typical failure modes of such structures are related to strong beam-weak column mechanisms.

The masonry infills are added to the RC frame, and the schematic representation of the case study frame with masonry infill is illustrated in Figure 1. Further details on the masonry infill characteristics are presented in a later section. The case-study building is designed as per the pre-seismic design codes ACI 318 (1989). The case study building has a bay width of 5.49 m and an interstory height of 3.66 m. The columns' cross-section

is 300 mm × 300 mm, while the cross-sectional dimension of beams is 230 mm × 460 mm. The compressive strength of the concrete is 24 MPa, while the yield strength of the reinforcements is 276 MPa. More details of the case study frame can be found in Aycardi *et al*., (1994) and Bracci *et al*., (1995). In addition, this study assumes a distribution of masonry infills with openings uniformly distributed throughout the RC frame, as shown in Figure 1.

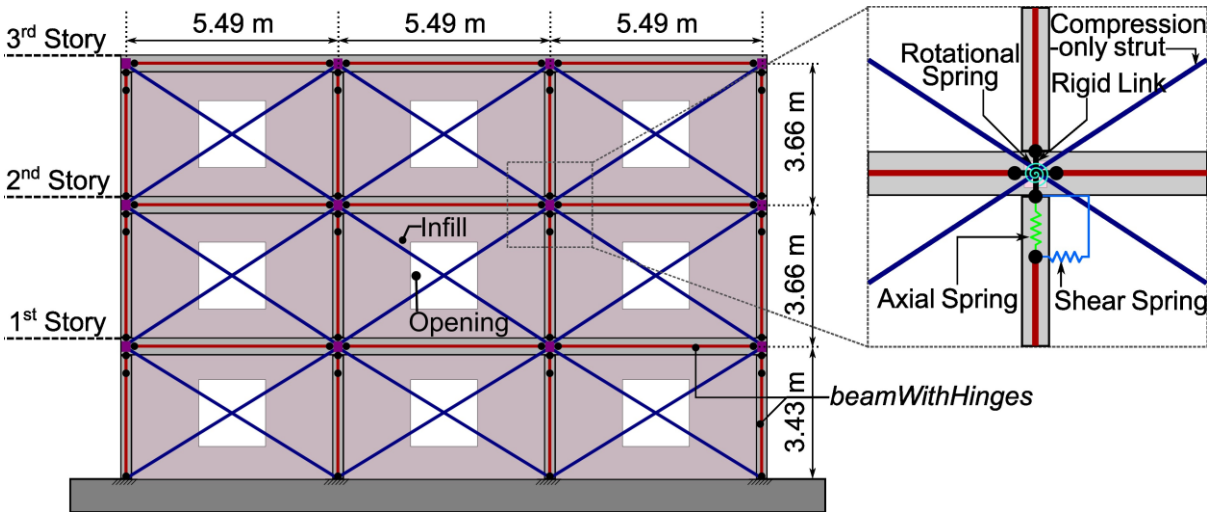

Figure 1. Schematic representation of case study frame with masonry infill.

3.1. Modeling of RC frame

A two-dimensional state-of-the-art FE model of the RC frame is developed in OpenSees (McKenna *et al.,* 2000). Beams and columns are modeled using the *beamWithHinges* element available in OpenSees. The concrete core and cover are modeled using the *Concrete02* material, whereas the reinforcements are modeled using the hysteretic material (*uniaxialMaterial Hysteretic*). Gravity loads are uniformly distributed along the beams, while the masses are concentrated at beam-column joints. *ZeroLength* shear springs are included at each column's top to capture possible shear failures that may be experienced by the columns in such low-ductility RC frames. Similarly, additional *ZeroLength* axial springs are introduced at each column's top to capture possible axial failures, as shown in Figure 1. *LimitState* uniaxial materials are used to define the shear and axial spring. More details on the modeling of the RC frame can be found in Freddi *et al.,* (2013), (2017) and (2021).

3.2. Modeling of masonry infill panel

This study utilizes a macro-modeling approach to model masonry infills in which masonry infill is idealized as compression-only equivalent diagonal struts, as shown in Figure 1 (Crisafulli *et al.,* 2000). The multilinear force-displacement back-bone curve of the masonry infill is developed based on the recommendation of Dolšek and Fajfar (2008). The peak force of the masonry infill is defined as follows:

$$F_m = 0.818\frac{L_{in}t_{in}f_{tp}}{C_I}\left(1+\sqrt{C_I^2+1}\right), \text{ where, } C_I = 1.925\frac{L_{in}}{H_{in}} \tag{4}$$

where f_{tp} and t_{in} are, respectively, the cracking strength estimated by diagonal compression test and thickness of the masonry infills; H_{in} *and* L_{in} are, respectively, the height and length of the masonry infills, as shown in Figure 2B. The parameter C_I accounts for the interaction between the masonry infill and the surrounding RC frame. The initial stiffness (K_i) of the masonry infill is determined according to Equation (5):

$$K_i = \frac{G_{in}L_{in}t_{in}}{H_{in}} \tag{5}$$

where G_{in} is the shear modulus of the masonry infill.

According to Dolšek and Fajfar (2008) the cracking force of the masonry infill (F_c) is taken as 60% of the peak force. The interstory drift corresponding to the peak strength (D_m) is taken as 0.15% for the masonry infill with openings for the windows. Successively, the interstory drift corresponding to the infill collapse (D_r) is taken as five times the drift corresponding to the peak force. This study also considers a residual force (F_r) of 5% of the peak force for the masonry infills. The force-displacement back-bone curve is represented in Figure 2A. The influence of the openings in the masonry infills is taken into account through the factor λ_0, (Equation (6)), which factors the peak force and the initial stiffness of the masonry infills.

$$\lambda_0 = 1 - \frac{1.5L_0}{L_{in}} \geq 0 \tag{6}$$

In the above equation, L_0 is the horizontal length of the opening, as shown in the Figure 2B. The horizontal length and the vertical height of the openings are assumed to be equal. In this study, the parameters that control the cyclic behavior of the masonry infill are adopted from Noh *et al.,* (2017).

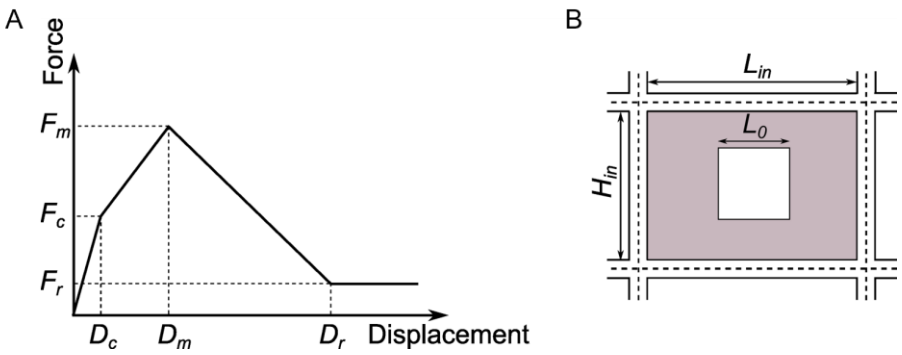

Figure 2. (A) Back-bone curve of masonry infills; (B) Masonry infill with opening.

The main material parameters controlling the back-bone curve of the masonry infill are the cracking strength (f_{tp}) and shear modulus (G_{in}). Masonry infills are commonly used in the construction industry, and they can significantly vary based on the type and material of the masonry unit, among others. This study uses a range of material properties typically found in literature. The f_{tp} is assumed to vary from 0.08 MPa to 0.55 MPa (Cobanoglu *et al.,* 2017; Hak *et al.,* 2012), the Young's Modulus is assumed to vary from 582 MPa to 4928 MPa (Cobanoglu *et al.,* 2017) and, consequently, the shear modulus (G_{in}) is estimated in the range from 242.5 MPa to 2053.3 MPa (by assuming Poisson ratio as 0.2).

4. Parametrized seismic fragility function

A Cloud Analysis is adopted herein to derive the probabilistic seismic demand models (Cornell *et al.,* 2002). The study uses a set of 240 unscaled ground motion records from Baker *et al.,* (2011) to perform the NLTHAs. The maximum interstory drift ratio (IDR_{max}) is assumed as the Engineering Demand Parameter (*EDP*) to monitor the global response of the structure. On the other hand, the average spectral acceleration (Sa_{avg}) is adopted as the intensity measure of choice. The samples of the demand obtained by the NLTHAs, together with the selected *IM* and samples of infill material properties, allow the definition of the seismic demand models and, subsequently, by comparing with building capacity estimates, the parameterized fragility functions are derived.

4.1. Probabilistic seismic demand models

Masonry infills typically experience substantial damages at low drift, leading to a reduction in the stiffness of the structure and the consequent fundamental time period elongation. To account for this period elongation, this study uses the average spectral acceleration as *IM*. The Sa_{avg} is the geometric mean of the spectral accelerations spanning over a period band (Baker and Jayaram, 2008; Eads *et al.,* 2015). In this study, the period band is considered to have a range from the fundamental time period of the stiffest building (*i.e.,* the infilled frame in its as-built state) to the fundamental time period of the more flexible building (*i.e.,* the infilled frame experiencing the largest stiffness reduction among the 240 seismic analyses). The expression to calculate Sa_{avg} is expressed in Equation 7.

$$Sa_{avg}\left(T_1,T_2,...T_u\right)=\left(\prod_{i=1}^{u}Sa\left(T_i\right)\right)^{1/u} \quad (7)$$

where $Sa(T_i)$ is the spectral acceleration at i^{th} time period; T_1, T_2,…, T_u are the periods of interest spanning from 0.13 s to 1.40 s with an interval of 0.01 s.

As mentioned in the earlier section, this study uses Latin Hypercube design of experiments to sample the material parameters of masonry infill. The parameters considered in this study includes cracking strength of the infill (f_{tp}) and shear modulus (G_{in}), and they are considered to vary from 0.08 MPa to 0.55 MPa for f_{tp} and 242.5 MPa to 2053.3 MPa for G_{in}. The considered infill parameters, *i.e.,* f_{tp} and G_{in}, are sampled to 240 design points (*i.e., n* equal to 240 in the present study), and infills' back-bone curves are developed as discussed in Section 3.2. Each infilled RC frame model is paired with one ground motion, NLTHAs are performed, and the samples for the demand are derived.

Successively fitted the surrogate demand model using a polynomial response surface model with first-order polynomial using the output parameter as IDR_{max} and input parameters as f_{tp}, G_{in}, and Sa_{avg} after performing logarithmic transformation on the parameters, and the regression coefficients are estimated. The Equation 8 below shows the expression for the fitted seismic demand model:

$$\ln(IDR_{\max}) = -1.38 - 0.42\times\ln(f_{tp}) - 0.55\times\ln(G_{in}) + 1.64\times\ln(Sa_{avg}) \quad (8)$$

The goodness-of-fit of the surrogate model is measured through Adjusted R^2 and Root Means Square Error (RMSE) by performing 10-fold cross validation. Higher values of Adjusted R^2 and lower values of RMSE show good fitting of the model to the data. In this seismic demand model fitting, the average Adjusted R^2 value is equal to 0.83, while the average RMSE value corresponds to 0.56. This shows the developed surrogate model fits the simulation data reasonably well and, hence, can be used with confidence. The subsequent section describes the seismic capacity estimation and successively the development of the parameterized fragility function using the developed surrogate model in conjunction with seismic capacity estimates.

4.2. Seismic capacity estimates

Nonlinear static pushover analysis is performed on the case study structure to map the global (*i.e., IDR*$_{max}$) to the local *EDPs,* such as the material strain of the cross section (Freddi *et al*., 2021; Rossetto *et al*., 2016). While the seismic demand model is parameterized in this study, however, the building capacity estimates are not. The mean value of f_{tp} and G_{in} are used for modeling the back-bone curve of the masonry infill, and the pushover analysis is performed with lateral loads proportional to the fundamental mode shape, as shown in Figure 3A. Figure 3B shows the pushover curve with base shear vs IDR_{max}. The pushover curve shows a reduction in the base shear after reaching the peak value due to damage experienced by the infills. Table 1 summarizes the four considered damage states (DSs), referred to as Slight, Moderate, Extensive, and Complete, along with their threshold estimates in terms of IDR_{max}. It is assumed that the capacity limits of the building follow a lognormal distribution with the median value listed in Table 1 and a dispersion of 0.3 (FEMA, 2003; Freddi *et al.,* 2021).

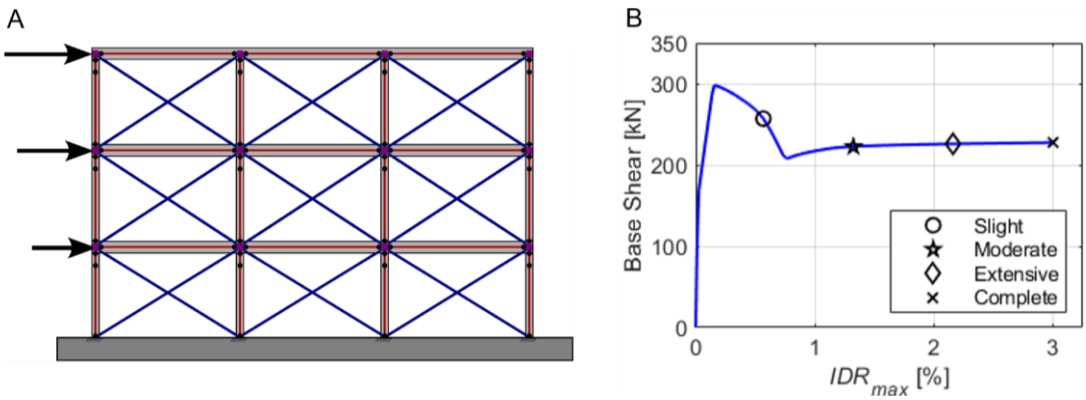

Figure 3. (*A*) *Schematic representation of pushover analysis.* (*B*) *Base shear vs IDR*$_{max}$ *plot and damage states (DSs) thresholds.*

Table 1. Description of damage states (DSs) and threshold values.

Damage states	Description	IDR_{max} (%)
Slight	50% of the columns on one story experienced yielding	0.57
Moderate	50% of the columns on one story experienced concrete crushing	1.32
Extensive	Average of Moderate and Complete	2.16
Complete	50% of the columns on one story experienced shear failure initiation	3.00

4.3. Parameterized fragility development

This study uses the logistic regression approach to derive the parameterized multidimensional fragility functions by utilizing the seismic demand model and building capacity estimates. The steps in the generation of the parameterized fragility function include the following: 1) a large number of demand vectors is generated by using the surrogate model developed by sampling from the input parameters **x**, along with the consideration of homoscedastic prediction error; 2) the DS threshold values are sampled for building capacity estimates; 3) a binary survival-failure vector of Bernoulli trials using the seismic demand and capacity is generated (Ghosh *et al.,* 2013; Rokneddin *et al.,* 2014); 4) the expression for the probability of failure in different DS is developed using the logistic regression technique using survive-failure vector according to the following expression:

$$P(DS \mid G_{in}, f_{tp}, Sa_{avg}) = \frac{e^{k_1 + k_2 \ln(G_{in}) + k_3 \ln(f_{tp}) + k_4 \ln(Sa_{avg})}}{1 + e^{k_1 + k_2 \ln(G_{in}) + k_3 \ln(f_{tp}) + k_4 \ln(Sa_{avg})}} \quad (9)$$

where k_1, k_2, k_3, and k_4 are the logistic regression coefficients. The regression coefficients of all DS are tabulated in Table 2.

Table 2. Logistic regression coefficients.

Damage states	Logistic regression coefficients			
	k_1	k_2	k_3	k_4
Slight	11.19	-1.23	-1.65	4.85
Moderate	8.46	-1.20	-1.60	4.69
Extensive	6.95	-1.18	-1.57	4.68
Complete	5.98	-1.17	-1.57	4.75

To show the variation of the seismic fragility of the building according to the Sa_{avg}, the parameterized multidimensional fragility function is converted to a unidimensional fragility function (i.e. conditioned only on Sa_{avg}) by holding the other parameters (*i.e.,* f_{tp} and G_{in}) at constant estimates. Figure 4A shows the seismic fragility of the building with respect to the Sa_{avg} for the Slight and Complete DSs by keeping the f_{tp} and G_{in} at their average values, *i.e.,* at 0.315 MPa and 1148 MPa, respectively.

Additionally, the influence of the variability of the strength parameter of masonry infills (f_{tp} = 0.08 MPa - 0.55 MPa) on the fragility curve conditioned on Sa_{avg} is shown through fragility bands in Figure 4A. It is worthwhile to note that an increase in the strength of the masonry infill increases the seismic performance of the structure. A similar trend is observed for other DSs but is not reported here for the sake of brevity.

Similarly, the influence of the variability of the elasticity parameter of the masonry infills (G_{in} = 242.5 MPa - 2053.3 MPa) on the fragility curve conditioned on Sa_{avg} is shown through fragility bands in Figure 4B. It is observed that an increase in the shear modulus leads to an increase in the seismic performance.

Figure 4C shows the seismic fragility of the infilled RC frame conditioned on f_{tp} by keeping the other two parameters, *i.e.,* the Sa_{avg} and G_{in}, at constant values, respectively, at 0.5 g and 1148 MPa. It is observed that when f_{tp} increases, the seismic fragility decreases for all DSs, and the same trend is observed in Figure 4A.

Figure 4D shows the seismic fragility of the infilled RC frame conditioned on G_{in} by keeping the other two parameters, *i.e.,* the Sa_{avg} and f_{tp}, at constant values, respectively, at 0.5 g and 0.315 MPa. It is observed that when G_{in} increases, the seismic fragility decreases, and the same is observed in Figure 4B.

Figure 5A shows the fragility curve for the Extensive DS conditioned on Sa_{avg} and f_{tp} by keeping G_{in} at its mean value (*i.e.*, 1148 MPa). Similarly, Figure 5B shows the fragility curve for the same DS conditioned on Sa_{avg} and G_{in} by keeping f_{tp} at its mean value (*i.e.*, 0.315 MPa). The same trend is observed in other DS but is not reported here for the sake of brevity. It is observed that the increase in the strength and shear modulus of the masonry infills leads to an increase in the seismic performance, hence reducing the seismic vulnerability of the infilled RC frame.

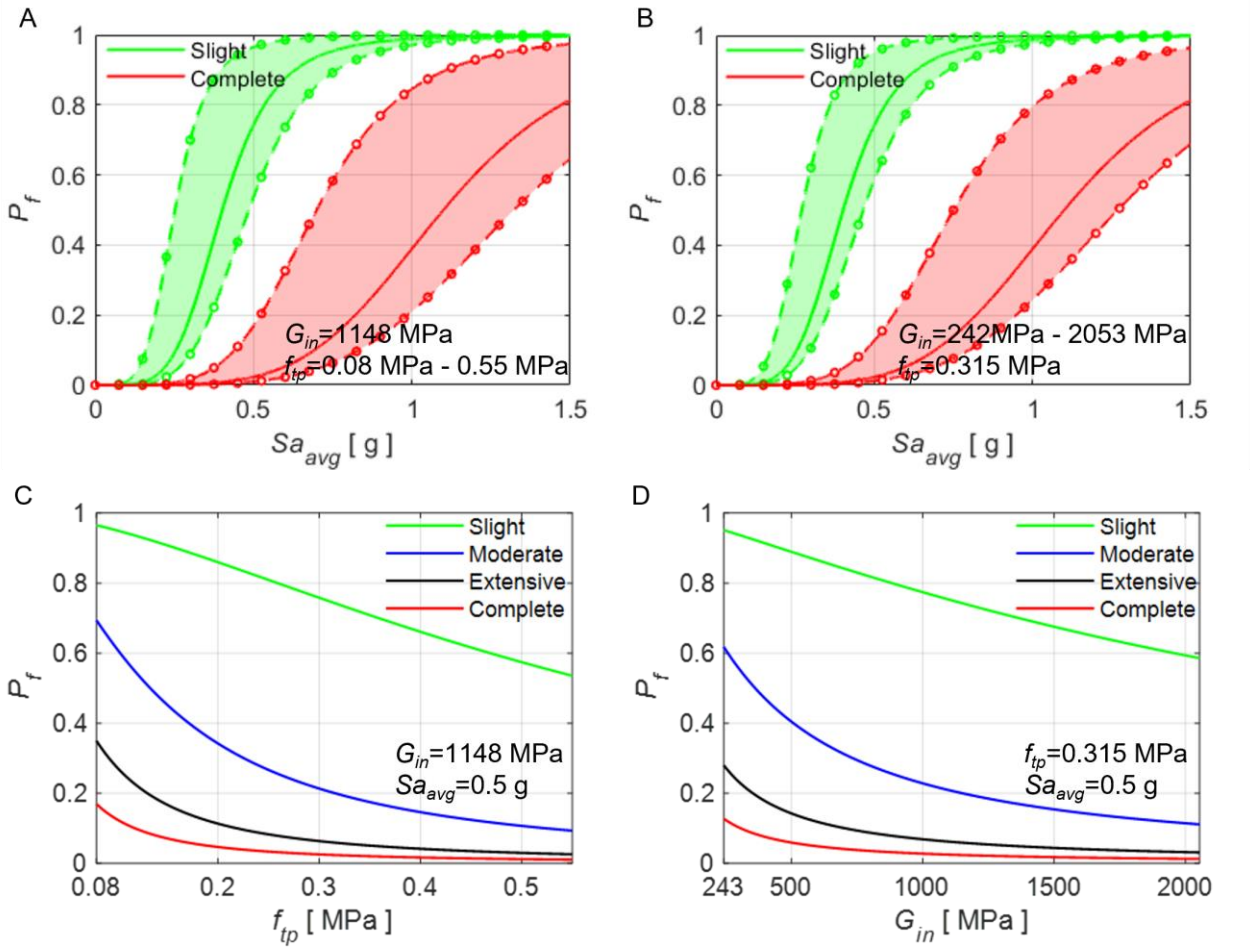

Figure 4. Seismic fragility of infilled RC frame: (A) Fragility band of f_{tp} with respect to Sa_{avg} with G_{in} constant; (B) Fragility band of G_{in} with respect to Sa_{avg} with f_{tp} constant; (C) Fragility with respect to f_{tp} with Sa_{avg} and G_{in} constant; (D) Fragility with respect to G_{in} with Sa_{avg} and f_{tp} constant.

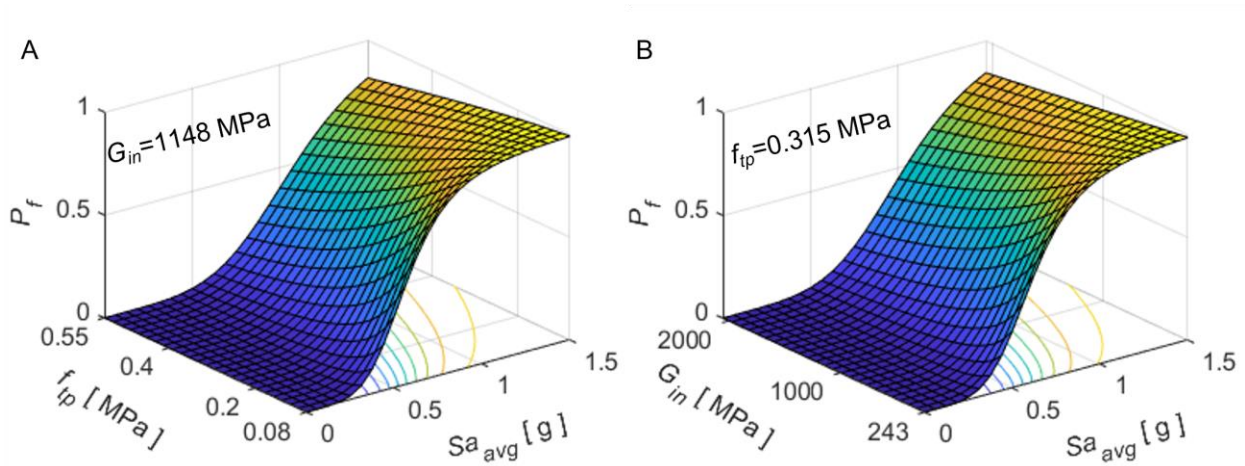

Figure 5. Seismic fragility of infilled RC frame: (A) Seismic fragility surface with respect to Sa_{avg} and f_{tp} with G_{in} constant; (B) Seismic fragility surface with respect to Sa_{avg} and G_{in} with f_{tp} constant.

It is worthwhile to note that the motivation to develop the metamodel is to gain computational efficiency with reasonable accuracy in seismic response and vulnerability prediction. Performing NLTHAs of 240 building models using a computer with Intel Xeon processor with 2.2 GHz and 64 GB RAM took approximately 27 hours, whereas the seismic response prediction using metamodeling took negligible computational time.

5. Conclusions

Masonry infilled RC frames represent a widely adopted construction typology worldwide. However, the brittle nature of the masonry infills often leads researchers to neglect their contribution in the analysis and design phase. However, recent literature shows that the strength and stiffness of the masonry infills can significantly affect the seismic performance of masonry infilled RC frames. This paper investigated the influence of the masonry infills' properties on the seismic performance of the masonry infilled RC frame by developing a novel framework based on surrogate models. Such models offer an effective alternative to provide comprehensive seismic performance assessments, simultaneously limiting the required computational effort.

A three-story, three-bay, low-ductility RC frame with masonry infill designed only for the gravity load is considered as the case study building. Two key material parameters controlling the behavior of the masonry infills are selected in this study, *i.e.,* the cracking strength (f_{tp}) and shear modulus (G_{in}). Latin Hypercube design of experiments is adopted to sample the material parameters of masonry infill, and a limited number of numerical simulations are performed. A polynomial response surface model with a first-order polynomial is used to derive a seismic demand model fitted using the input and output response parameters from the numerical simulations. The results show average Adjusted R^2 and RMSE values of 0.83 and 0.56, respectively. Nonlinear static pushover analysis is performed to define damage state thresholds of the structure based on global engineering demand parameters (*i.e.,* maximum interstory drift ratio). The seismic demand model and DS thresholds allow for deriving the parameterized fragility function through logistic regression techniques. The established parameterized multidimensional fragility function shows how the seismic vulnerability of the building is affected by the material properties of the masonry infills and how it reduces while increasing the cracking strength and shear modulus of the masonry infill. Additionally, the present paper shows how the parameterized multidimensional fragility function represents an easily accessible tool to evaluate the variability of the seismic vulnerability with respect to selected parameters. The novel framework proposed in this study can be extended to additional parameters and different structures to develop comprehensive and generalized parameterized multidimensional fragility functions for seismic performance evaluation and vulnerability assessment. The future work of the present study also lies in adopting advanced metamodeling techniques for the development of seismic demand models, the development of parameterized models for building capacity estimates, and considering different categories of infills, among others.

6. Acknowledgment

The funding from the Science and Engineering Research Board (statutory body under the Department of Science and Technology, India) through Grant No. CRG/2021/000777 for this work is greatly acknowledged by the authors.

7. References

ACI Committee 318 (1989). *Building Code Requirements for Reinforced Concrete and Commentary (ACI 318-89/ACI 318R-89)*.

Alizadeh R., Allen J. K., Mistree F. (2020). Managing computational complexity using surrogate models: a critical review, *Research in Engineering Design*, 31(3): 275–298.

Aycardi L. E., Mander J. B., Reinhorn A. M. (1994). Seismic resistance of reinforced concrete frame structures designed only for gravity loads: Experimental performance of subassemblages, *ACI Materials Journal*, 91(5): 552–563.

Baker J. W., Jayaram N. (2008). Correlation of spectral acceleration values from NGA ground motion models, *Earthquake Spectra*, 24(1): 299–317.

Baker J. W., Lin T., Shahu S. K., Jayaram N. (2011). New Ground Motion Selection Procedures and Selected Motions for the PEER Transportation Research Program, *Pacific Earthquake Engineering Research Center*.

Blasi G., Perrone D., Aiello M. A. (2018). Fragility functions and floor spectra of RC masonry infilled frames: influence of mechanical properties of masonry infills, *Bulletin of Earthquake Engineering*, 16(12): 6105–6130.

Bracci J. M., Reinhorn A. M., Mander J. B. (1995). Seismic resistance of reinforced concrete frame structures designed for gravity loads: performance of structural system, *ACI Materials Journal*, 92(5): 597–609.

Campione G., Cavaleri L., Macaluso G., Amato G., Di Trapani F. (2015). Evaluation of infilled frames: an updated in-plane-stiffness macro-model considering the effects of vertical loads, *Bulletin of Earthquake Engineering*, 13(8): 2265–2281.

Cavaleri L., Di Trapani F. (2014). Cyclic response of masonry infilled RC frames: Experimental results and simplified modeling, *Soil Dynamics and Earthquake Engineering*, 65: 224–242.

Cobanoglu B., Aldemir A., Demirel İ. O., Binici B., Canbay E., Yakut A. (2017). Seismic Performance Assessment of Masonry Buildings Using In Situ Material Properties, *Journal of Performance of Constructed Facilities*, 31(4): 1–12.

Cornell C. A., Jalayer F., Hamburger R. O., Foutch D. A. (2002). Probabilistic Basis for 2000 SAC Federal Emergency Management Agency Steel Moment Frame Guidelines, *Journal of Structural Engineering*, 128: 526–533.

Crisafulli F. J., Carr A. J., Park R. (2000). Analytical modelling of infilled frame structures - A general review, *Bulletin of the New Zealand Society for Earthquake Engineering*, 33(1): 30–47.

Di Sarno L., Freddi F., D'Aniello M., Kwon O. S., Wu J. R., Gutiérrez-Urzúa F., … Strepelias E. (2021). Assessment of existing steel frames: Numerical study, pseudo-dynamic testing and influence of masonry infills, *Journal of Constructional Steel Research*, 185.

Dolšek M., Fajfar P. (2008). The effect of masonry infills on the seismic response of a four-storey reinforced concrete frame - a deterministic assessment, *Engineering Structures*, 30(7): 1991–2001.

Eads L., Miranda E., G. Lignos Dimitrios (2015). Average spectral acceleration as an intensity measure for collapse risk assessment, *Earthquake Engineering & Structural Dynamics*, 44: 2057–2073.

Elwood K. J., Moehle J. P. (2005). Drift capacity of reinforced concrete columns with light transverse reinforcement, *Earthquake Spectra*, 21(1): 71–89.

Esteghamati Z. M., Flint M. M. (2021). Developing data-driven surrogate models for holistic performance-based assessment of mid-rise RC frame buildings at early design, *Engineering Structures*, 245: 112971.

FEMA (2003). *HAZUS-MH MR4 Technical Manual-Earthquake Model*.

Freddi F., Ghosh J., Kotoky N., Raghunandan M. (2021). Device uncertainty propagation in low-ductility RC frames retrofitted with BRBs for seismic risk mitigation, *Earthquake Engineering and Structural Dynamics*, 50(9): 2488–2509.

Freddi F., Padgett J. E., Dall'Asta A. (2017). Probabilistic seismic demand modeling of local level response parameters of an RC frame, *Bulletin of Earthquake Engineering*, 15(1): 1–23.

Freddi F., Tubaldi E., Ragni L., Dall'Asta A. (2013). Probabilistic performance assessment of low-ductility reinforced concrete frames retrofitted with dissipative braces, *Earthquake Engineering and Structural Dynamics*, 42(7): 993–1011.

Ghosh J., Padgett J. E., Dueñas-Osorio L. (2013). Surrogate modeling and failure surface visualization for efficient seismic vulnerability assessment of highway bridges, *Probabilistic Engineering Mechanics*, 34: 189–199.

Hak S., Morandi P., Magenes G., Sullivan T. J. (2012). Damage control for clay masonry infills in the design of RC frame structures, *Journal of Earthquake Engineering*, 16(SUPPL. 1): 1–35.

Martinelli E., Lima C., De Stefano G. (2015). A simplified procedure for Nonlinear Static analysis of masonry infilled RC frames, *Engineering Structures*, 101: 591–608.

McKay M. D., Beckman R. J., Conover W. J. (1979). Comparison of three methods for selecting values of input variables in the analysis of output from a computer code, *Technometrics*, 21(2): 239–245.

McKenna F., Fenves G. L., Scott M. H. (2000). Open System for Earthquake Engineering Simulation, *Pacific Earthquake Engineering Research Center*.

Mosalam K. M., Günay S. (2015). Progressive collapse analysis of reinforced concrete frames with unreinforced masonry infill walls considering in-plane/out-of-plane interaction, *Earthquake Spectra*, 31(2): 921–943.

Mucedero G., Perrone D., Monteiro R. (2023). Seismic risk assessment of masonry-infilled RC building portfolios: impact of variability in the infill properties, *Bulletin of Earthquake Engineering*, 21(2): 957-995.

Noh N. M., Liberatore L., Mollaioli F., Tesfamariam S. (2017). Modelling of masonry infilled RC frames subjected to cyclic loads: State of the art review and modelling with OpenSees, *Engineering Structures*, 150: 599–621.

Paulay T., Priestley M. J. N. (1992). *Seismic design of reinforced concrete and masonry buildings*. New York: John Wiley & Sons.

Rao A., Dutta D., Kalita P., Ackerley N., Silva V., Raghunandan M., … Dasgupta K. (2020). Probabilistic seismic risk assessment of India, *Earthquake Spectra*, 36(1_suppl): 345–371.

Rokneddin K., Ghosh J., Dueñas-Osorio L., Padgett J. E. (2014). Seismic reliability assessment of aging highway bridge networks with field instrumentation data and correlated failures, II: Application, *Earthquake Spectra*, 30(2): 819–843.

Rossetto T., Elnashai A. (2003). Derivation of vulnerability functions for European-type RC structures based on observational data, *Engineering Structures*, 25(10): 1241–1263.

Rossetto T., Gehl P., Minas S., Galasso C., Duffour P., Douglas J., Cook O. (2016). FRACAS: A capacity spectrum approach for seismic fragility assessment including record-to-record variability, *Engineering Structures*, 125: 337–348.

Sattar S., Liel A. B. (2016). Seismic performance of nonductile reinforced concrete frames with masonry infill walls - I: Development of a strut model enhanced by finite element models, *Earthquake Spectra*, 32(2): 795–818.

Wu J. R., Di Sarno L., Freddi F., D'Aniello M. (2022). Modelling of masonry infills in existing steel moment-resisting frames: Nonlinear force-displacement relationship, *Engineering Structures*, 267: 114699.